Eleventh International Conference on CFD in the Minerals and Process Industries
CSIRO, Melbourne, Australia
7-9 December 2015

A DISSIPATIVE PARTICLE DYNAMICS MODEL OF YIELD STRESS FLUIDS: APPLICATION TO HIGHLY CONCENTRATED SEDIMENT MIXTURES

Khoa LE-CAO[1*], Nhan PHAN-THIEN[1, 2] and Boo Cheong KHOO[1, 2]
[1]Keppel-NUS Corporate Laboratory
[2] Department of Mechanical Engineering, Faculty of Engineering,
National University of Singapore, Singapore
*Corresponding author, E-mail address: mpeleck@nus.edu.sg

ABSTRACT

This paper is concerned with the numerical modelling of yield stress fluids using a particle-based simulation technique, known as dissipative particle dynamics (DPD), in which both the sediment and surrounding fluid are modelled by particles undergoing their Newton's 2nd law motion. This technique satisfies conservation of mass and momentum and it has been applied successfully for a number of problems involving complex-structure fluids, such as polymer solutions, suspensions of rigid particles, droplets, and biological fluids. In the proposed model, two DPD species, one standard DPD to represent the solvent, with only repulsive conservative force, and the other, with repulsive force at short range and attractive force at long range to represent sediment particles. The advantage of the method is that the multiphase properties of the system are reconstructed, and thus there is no requirement of the constitutive equations. Numerical results show that the proposed model can represent some behaviours of highly concentrated sediment mixtures.

NOMENCLATURE

Greek Symbols

γ	Magnitude of the dissipative force
μ	Dynamic viscosity
ξ	Gaussian variable with zero mean
ρ	Mass density
σ	Magnitude of the random force
τ_y	Yield stress

Latin Symbols

A	Coefficient of repulsive component
a	Conservative force strength
B	Coefficient of attractive component
$\mathbf{D}$	Strain rate tensor
k_BT	Boltzmann temperature
m	Mass of a DPD particle
N	Number of DPD particles
N_{DPD-a}	Number density of DPD-a
N_{DPD-b}	Number density of DPD-b
n	Control parameter
$\boldsymbol{r}_i$	Position of a DPD particle
r_{cr}	Cut-off radius of repulsive component
r_{ar}	Cut-off radius of attractive component
$\mathbf{S}$	Extra stress tensor
$\mathrm{v_i}$	Velocity of a DPD particle
w_r^c	Weight function of repulsive component
w_a^c	Weight function of attractive component

Sub/superscripts

i	Particle *i*th
ij	Particle *j to i*
C	Conservative force term
D	Dissipative force term
R	Random force term

INTRODUCTION

Since mixtures at high volume fractions (including clay and sediments) behave like a yield-stress fluid (i.e. it is able to flow only if it is submitted to a stress above some critical value), we devoted some research effort in modelling of these fluids. In continuum mechanics, such materials are modelled by rheological constitutive equations (e.g. Bingham models). These equations are then transformed into sets of algebraic equations by means of discretisation. However, it is known that Bingham models may have the discontinuity in the constitutive relations. Papanastasiou [Papanastasiou (1987)] proposed a modified version of Bingham model to overcome this numerical difficulties. The non-discontinuity Bingham model can be written as:

$$\boldsymbol{S} = 2\left\{\mu + \frac{\tau_y\left[1-\exp\left(-n|II_{\boldsymbol{D}}|^{1/2}\right)\right]}{|II_{\boldsymbol{D}}|^{1/2}}\right\}\mathbf{D} \tag{1}$$

where $\mathbf{S}$ is the extra stress, $\mathbf{D}$ strain rate tensor, $II_{\boldsymbol{D}}$ the second invariant of $\mathbf{D}$, τ_y yield stress value, and n a parameter. At high strain rate, this model results in $\boldsymbol{S} = 2\mu\boldsymbol{D}$, a Newtonian fluid with viscosity μ. At low strain rate, viscosity becomes $\mu + n\tau_y$. Consequently, for large n, this fluid model appears to have a yield stress.

In the last two decades the DPD method [Hoogerbrugge and Koelman (1992)] has been developed as an alternative and promising mesoscopic approach for modelling a complex fluid. Different from schemes based on discretisations of macroscopic continuum equations, the DPD method is based on coarse-grained models and Langevin equations. Its formulation is derived from the view that each DPD particle is a coarse-grained representation of a group of fluid particles. DPD method often looks similar to Molecular Dynamics (MD). However, DPD particles interact through a soft potential and thus the simulation can be carried out on length and time scales far beyond those associated with MD. It has been show in [Español (1995)] that mean quantities formed from the microstate of a DPD system (positions and velocities) satisfy the conservation laws (mass and momentum). Therefore, the method may be applicable to problems of any scale and regarded as a

particle-based method for solving continuum problems [Phan-Thien (2013)]. There are many applications of DPD method and its variants to simulation of complex fluids have been reported e.g. sphere colloidal suspensions [Koelman and Hoogerbrugge (1993); Pan et al. (2010)], colloidal suspensions of spheres, rods, and disks [Boek et al. (1997)], ferromagnetic colloidal suspension [Li (2015)], soft matter and polymeric applications [Moeendarbary (2010)], droplet modelling [Pan et al. (2014)] and lipid bilayer [Sevink and Fraaije (2014)].

In this research, the DPD method is modified to investigate the rheology of sediment mixtures under shear flows and Poiseuille flows. We treat both the fluid and the sediment as an assembly of DPD particles, with distinct properties. The relation of stress and shear rate is studied for these mixtures under different DPD parameters. Numerical results show that the obtained DPD data can be fitted well to that of Papanastasiou's yield stress model. The significance of our method is that the constitutive framework is fully specified with DPD microstructure that goes into the description of the proposed model.

A TYPICAL DPD FLUID MODEL

In DPD method, the fluid and all its component phases (if have) are defined by the assemblage of N particles, each of mass $m_i, \mathrm{i} = 1, \ldots, \mathrm{N}$, located at position r_i, with velocity v_i, with an assumption of identical mass $m_i = m$. The DPD particles interact with each other and undergo their Langevin motions which can be written as [Marsh (1998)]:

$$\frac{d\boldsymbol{r}_i}{dt} = \boldsymbol{v}_i, \quad m\frac{d\boldsymbol{v}_i}{dt} = \boldsymbol{f}_i + \boldsymbol{F}_e \tag{2}$$

where $\mathbf{F}_\mathrm{e}$ is external forces on particle i (e.g. gravity force), $\boldsymbol{f}_i = \sum_{j\neq i}\boldsymbol{F}_{ij}$ the interaction force on particle i by particle j, pairwise additive. It is note that the sum runs over all other particles ($\boldsymbol{F}_{ii} = 0$), within a certain cut-off radius r_c. The interaction force $\boldsymbol{F}_{ij}$consists of three parts, a conservative force, $\boldsymbol{F}_{ij}^C$, a dissipative force, $\boldsymbol{F}_{ij}^D$, and a random force, $\boldsymbol{F}_{ij}^R$:

$$\boldsymbol{F}_{ij} = \boldsymbol{F}_{ij}^C + \boldsymbol{F}_{ij}^D + \boldsymbol{F}_{ij}^R \tag{3}$$

Expressions of interaction forces are listed in **Table 1** in which a_{ij} is conservative force strength; $\boldsymbol{r}_{ij} = \boldsymbol{r}_i - \boldsymbol{r}_j; r_{ij} = |\boldsymbol{r}_{ij}|$; $\hat{\boldsymbol{r}}_{ij} = \frac{\boldsymbol{r}_{ij}}{|\boldsymbol{r}_{ij}|}; w^C, w^D, w^R$ weight functions of conservative, dissipative and random forces, respectively; $\boldsymbol{v}_{ij} = \boldsymbol{v}_i - \boldsymbol{v}_j$; s a constant, γ a coefficient related to system viscosity; ξ_{ij} a Gaussian variable with zero mean and variance equal to δt^{-1}, where δt is the time step, and σ is the magnitude of the random forces.

Fluid properties

The interested domain is divided by Cartesian grids and local data are collected in each cell of the grid. The flow properties including fluid density ρ, stress $\boldsymbol{S}$ and viscosity μ are calculated by appropriate averages over all sampled data in each cell. Fluid density is defined as

$$\rho(\boldsymbol{r}, t) = m\langle\textstyle\sum_i \delta(\boldsymbol{r} - \boldsymbol{r}_i)\rangle\,, \tag{4}$$

and stress tensor components are calculated by Irving-Kirkwood expression ([Irving and Kirkwood (1950)]) as follows

$$\boldsymbol{S} = -\frac{1}{V}\langle\textstyle\sum_i m\boldsymbol{u}_i\boldsymbol{u}_i + \frac{1}{2}\sum_i\sum_{j\neq i}\boldsymbol{r}_{ij}\boldsymbol{f}_{ij}\rangle, \tag{5}$$

where V is the volume of the bin and $\boldsymbol{u}_i$ are the peculiar velocity components of particle i and the symbol $\langle\ \rangle$ indicates a long time average for many iteration steps. For Newtonian fluid, viscosity can be found by using the relation between stress components and strain rate $\mu = \boldsymbol{S}/\dot{\gamma}$. It is noted that one can adjust viscosity value by changing the magnitude or weight functions of dissipative forces . It is important to mention that these quantities have been shown to satisfy conservation laws [Marsh (1998)]:

$$\frac{\partial}{\partial t}\rho(\boldsymbol{r}, t) + \boldsymbol{\nabla}.\big(\rho(\boldsymbol{r}, t)\boldsymbol{u}(\boldsymbol{r}, t)\big) = 0, \quad \boldsymbol{\nabla} = \partial/\partial\boldsymbol{r} \tag{6}$$

$$\frac{\partial}{\partial t}\big(\rho(\boldsymbol{r}, t)\boldsymbol{u}(\boldsymbol{r}, t)\big) + \nabla.\big(\rho(\boldsymbol{r}, t)\boldsymbol{u}(\boldsymbol{r}, t)\boldsymbol{u}(\boldsymbol{r}, t)\big) = \nabla.\mathbf{S} \tag{7}$$

Thus, DPD may be regarded as a particle-based method for solving continuum flow problems (6)-(7). Yield stress behaviour of highly concentrated sediment mixtures may be captured by this particle-based method. The nonlinear relationship between stress and strain rate needs not to be specified *a-priori*, but can be obtained after post-processing step. The main objective is how to identify the constitutive relation from the microstructure.

DPD COHESIVE MODEL FOR YIELD STRESS FLUID

After some investigations, we proposed a DPD model consisting of two species of DPD, DPD-a, a normal DPD with repulsive force, represents the solvent and DPD-b, a DPD with long range attractive and short range repulsive force, represent a clay-like sediment particle. The modified version of DPD-b is developed by adding a long-range attractive component to the conservative forces. It is important to mention that a DPD-b (sediment particle) attracts some of DPD-a (solvent) within its effective radius (Figure 1).

$\mathbf{F}_{\mathrm{ij}}$	Weight functions	Forms
$\boldsymbol{F}_{ij}^C$	$w^C(r_{ij}) = 1 - r_{ij}/r_c$	$a_{ij}w^C\hat{\boldsymbol{r}}_{ij}$
$\boldsymbol{F}_{ij}^D$	$w^D(r_{ij}) = (1 - r_{ij}/r_c)^s$	$-\gamma w^D(\hat{\boldsymbol{r}}_{ij}\cdot\boldsymbol{v}_{ij})\hat{\boldsymbol{r}}_{ij}$
$\boldsymbol{F}_{ij}^R$	$w^R(r_{ij}) = \sqrt{w^D(r_{ij})}$	$\sigma w^R\xi_{ij}\hat{\boldsymbol{r}}_{ij}$

Table 1: List of interaction forces and their formulas. It is important to note that the balance between dissipative and random forces must obey the fluctuation-dissipation theorems $\sigma = \sqrt{2\gamma k_B T}$ [Marsh (1998)].

Conservative force $\boldsymbol{F}_{ij}^c$ of DPD-b is calculated by taking derivative with respect to r of a potential similar to Lennard-Jones potential with attractive and repulsive terms [Liu and Huang (2006)].

$$\boldsymbol{F}_{ij}^c = -a_{ij}\big(Aw_r^c(r, r_{cr}) - Bw_a^c(r, r_{ca})\big)\hat{\mathbf{r}}_{\mathrm{ij}} \tag{8}$$

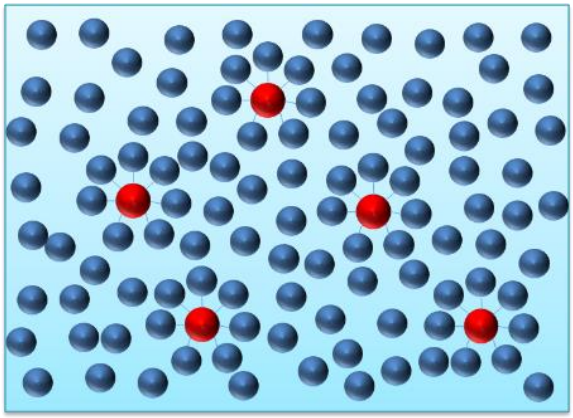

Figure 1: Microstructure of the proposed model: two species of DPD (DPD-a (blue colour)) and DPD-b (red colour)). A DPD-b attracts some DPD-a within its long range radius and repulses other DPD-b and DPD-a in short ranges radius.

where A and B are coefficient of $w_r^c(r, r_{cr})$ and $w_a^c(r, r_{ca})$, respectively. r_{cr} is cut-off radius of repulsive component and r_{ca} is that of attractive component and

$$w_r^c(r, r_{cr}) = \begin{cases} -12\frac{r}{r_{cr}^2} + \frac{18r^2}{r_{cr}^3}, r < \frac{r_{cr}}{2} \\ -\frac{3}{2r_{cr}}\left(2 - 2\frac{r}{r_{cr}}\right)^2, \frac{r_{cr}}{2} < r < r_{cr} \\ 0, r > r_{cr} \end{cases}$$

and

$$w_r^c(r, r_{ca}) = \begin{cases} -12\frac{r}{r_{ca}^2} + \frac{18r^2}{r_{ca}^3}, r < \frac{r_{ca}}{2} \\ -\frac{3}{2r_{ca}}\left(2 - 2\frac{r}{r_{ca}}\right)^2, \frac{r_{ca}}{2} < r < r_{ca} \\ 0, r > r_{ca}. \end{cases}$$

It can be seen from Figure 2 that the conservative force between two different species particles is repulsive (the positive part) when their separation distance is less than the value of radius r (e.g. 0.5952 with $A = 2, B = 1, r_{cr} = 0.8, r_{ca} = 1$) and when their separation distance falls in the range between 0.5952 and 1 this force describes a long range attraction (the negative part). At the initial stage, purely repulsive conservative forces (i.e. B = 0 in (8) for DPD-b) are applied for both type particles; DPD fluid is thus simply Newtonian. When the attractive components in conservative forces of DPD-b are turned on, a structure is formed result in high DPD fluid's resistance to shear stress. In next section, numerical results are reported to support the proposed model.

NUMERICAL RESULTS

The parameters of the proposed model will be obtained in Couette flows and then verified in Poiseuille flows. The simulation is carried out on a 3D cubic domain having side length of 10 unit with the following DPD parameters: $m_i = 1$, $a_{ij} = 18.75, \gamma = 4.5, r_{cr} = 0.8, r_{ca} = 1.0$.

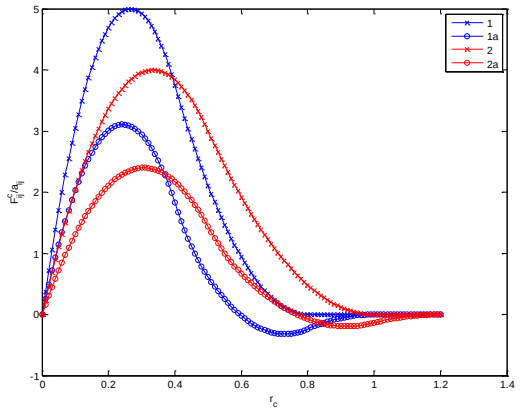

Figure 2: Conservative forces with repulsion only (-x, DPD-a), $r_c = 1.2$ (2) and $r_c = 1.0$ (1) and with short range repulsion and long range attraction (-o, DPD-b), $r_c = 1.2$ (2a) and $r_c = 1.0$ (1a).

For conservative force of DPD-b, we consider the strength of repulsive part and attractive part (Figure 2 - function 2a) in the range of A = {3, 4, 5} and B = {1.5, 2, 2.5}, respectively. For dissipative force, in a modified version of DPD systems introduced by [Fan et al. (2006)], two parameters are set as $1.0 \leq r_c \leq 1.5$ and $s = \frac{1}{2}$, in order to enhance the dynamic response. Similar to [Fan et al. (2006)], we use $s = \frac{1}{2}$, and fix the cut-off radius value at 1.0 for both DPD-a and DPD-b. Number density of DPD-a, N_{DPD-a}, is 6 and that of DPD-b, N_{DPD-b}, is 4. The simulation is run with 100,000 time steps and a unique time step 10^{-2} is chosen for all simulations. Periodic boundary conditions are applied in x- and y-direction, i.e. particles that have passed the interested domain at one face reappear in the domain at the opposite face and therefore one can effectively deals with a large (infinite) DPD system. In z-direction, solid walls are represented by three layers of frozen particles. It is known that conventional solid boundary models for DPD lead to slip boundary even at moderate Reynolds flow. To reduce this, wall wetting model [Arienti et al. (2011)] are employed in the Couette and Poiseuille flows to mimic hydrophilic behaviours. In all the following simulations, the Verlet integration algorithm is employed to solve equation (2).

Prepare the fluid: premix vs non premix

A pre-processing program is used to generate a system which consists of N particles with masses m characterised by the positions $\boldsymbol{x}_i, i = \{1, N\}$. The particle list is constituted from three segment including wall particle, matrix particle and suspended particle zones. For initial configuration, the simulation box is filled with DPD-b particles in the bottom and with DPD-a particles on top (Figure 3a). In addition, the initial distribution of these particles do not satisfy a thermodynamic equilibrium state. In pre-processing program a mixing procedure is thus applied. At the beginning of the mixing procedure, the particles are allowed to move freely until a thermodynamic equilibrium state is reached and then a body force $\mathbf{F}_e = (0.2,0,0)$ is applied around hundred thousand time steps to mix DPD-a and DPD-b. Figure 3b shows that after mixing conservative interactions produced a uniform DPD-b dispersion. The particle configuration are written in a data file which is then read by the DPD solver program.

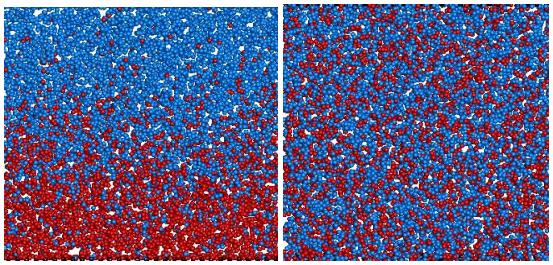

Figure 3: (a) Initial configuration of DPD-a (red sphere) and DPD-b (blue sphere) – **(b)** Uniform distribution of two species of DPD, which are obtained over the period of 100000 time steps.

Couette flow

The shear rate in the range of 0.01 to 1.64 is considered. The viscosity as a function of shear rate is plotted in Figure 4. DPD results show that viscosity is decreased dramatically from 238 at shear rate 0.01 to 17.68 at shear rate 1.64. We choose to compare the DPD prediction with the modified Bingham model (1) ([Papanastasiou (1987)]). Figure 5 shows the plot of average shear stress with different values of shear rates. It can be seen that the data

obtained by DPD model with volume fraction of DPD-b $\frac{N_{DPD-b}}{(N_{DPD-a}+N_{DPD-b})} = 0.4$ match to Papanastasiou's model, with a low-shear viscosity of 238, a high-shear viscosity of 17.68, and a yield stress of 8 (all dimensionless).

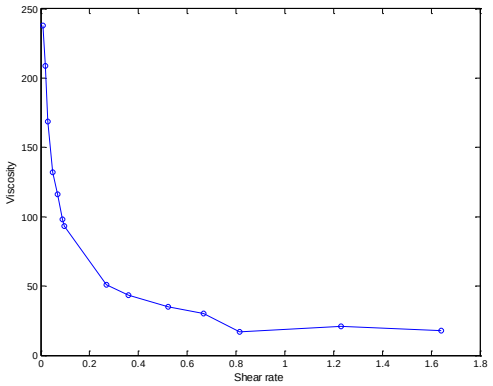

Figure 4: Viscosity plotted as a function of shear rate.

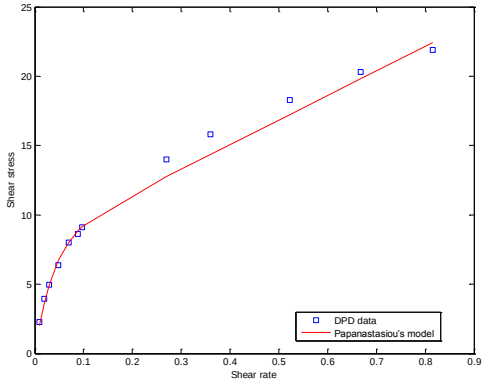

Figure 5: The obtained DPD data can be fitted well to Papanastasiou's model (1), with a low-shear viscosity of $\mu + n\tau_y$ = 238 (slope of the rheogram when shear rate smaller than 0.1), a high-shear viscosity of $\mu =$ 17.68 (slope of the rheogram when shear rate larger than 0.1), and a yield stress of $\tau_y = 8$ (all dimensionless).

Non-linear shear stress – shear rate as a function of k_BT and the repulsive force (A) are plotted in Figure 6 and in Figure 7. For first cases, a non-linear shear stress – shear rate relation is observed and low shear rate viscosity increases as k_BT is reduced. For second case, the whole curve is shifted up (increasing yield stress) when the strength of repulsive forces A are increased.

Couette flow results concerning the velocity field are presented in Figure 8, where DPD-b particle fraction is 40%. It can be seen that profiles of linear velocity are obtained even at low shear rate. The linear velocity profile can be explained by the distributions of two species of DPD over the domain. There is no phase separation in this solvent-sediment mixture under applied shear rates over the period of 100000 time steps.

Poiseuille flow

For verification, the same DPD fluid which match to Papanastasiou's model, (high-shear viscosity $\mu + n\tau_y =$ 238, a high-shear viscosity $\mu = 17.68$, and a yield stress $\tau_y = 8$) is placed between two parallel plates to simulate Poiseuille flow. A body force is applied to each fluid particle in x-direction, and this drives the flow. The periodic boundary conditions are applied to fluid boundaries in the x- and y- directions. Figure 9 compares the curve of shear stress versus shear rate calculated from shear flow and Poiseuille flow. Good agreement is achieved. The development of velocity profiles is shown in Figure 10. It can be seen that the DPD velocity profile is no longer parabolic. It flattens in the region around the centre and steepens in the region near the wall. The DPD model results are comparable to those of analytical solutions of the continuum model.

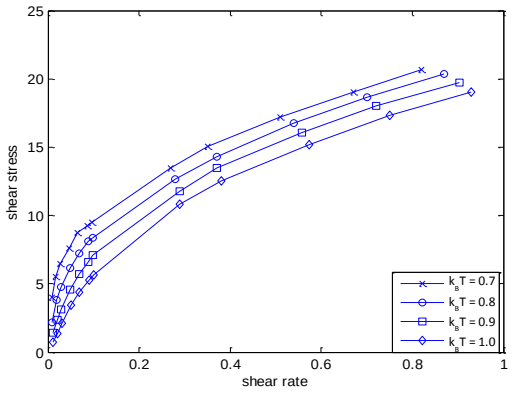

Figure 6: Non-linear shear stress – shear rate behaviour at different values of $k_BT = \{0.7, 0.8, 0.9, 1.0\}$ from top to bottom.

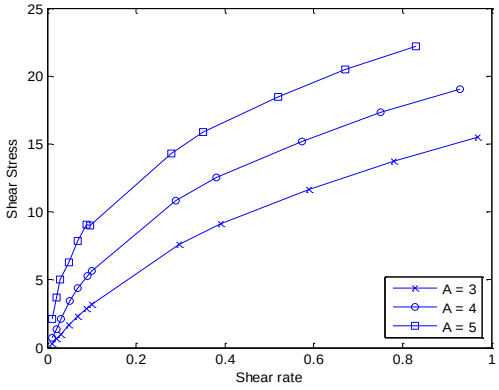

Figure 7: Non-linear shear stress – shear rate behaviour at different values of repulsive term coefficient in equation (8), $A = \{3, 4, 5\}$, from bottom to top.

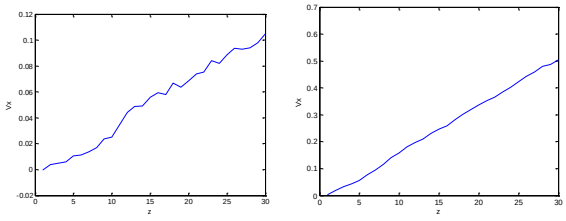

(a) (b)

Figure 8: Shear flow, linear velocity profiles at shear rate {0.01 (a), 0.05 (b)}.

CONCLUSION

In this article, a numerical model based on Dissipative Particle Dynamics method for yield stress fluids have been developed. The constitutive framework is fully specified with the microstructure that goes into the description of the DPD model. In spite of its simplicity, the present model is

able to produce some predictions of the nonlinear relation between shear stress and shear rate in viscometric flows. The normalised velocity profile of DPD fluid in the Poiseuille flow is similar to that obtained by Papanastasiou's model. Non-viscometric problems (e.g. contraction expansion flows or elongational flows) and particle interaction studies (e.g. pairwise radial distribution function of the different types of particles (DPD-a, DPD-b)) will be carried out and reported in future works. With the conservation of mass and momentum properties, the proposed DPD model may be regarded as a particle-based method for solving complex-structure fluids. However, that is still difficult to identify the direct relation to material properties (e.g. yield stress, viscosity) in physical unit and DPD unit. In Smoothed DPD method [Español and Revenga (2003)], one of DPD variants, this issue can be solved by choosing interaction forces with a specific form which comprised from the Smooth Particle Hydrodynamics discretisation. A similar technique will be needed in further studies to implement the proposed yield stress model.

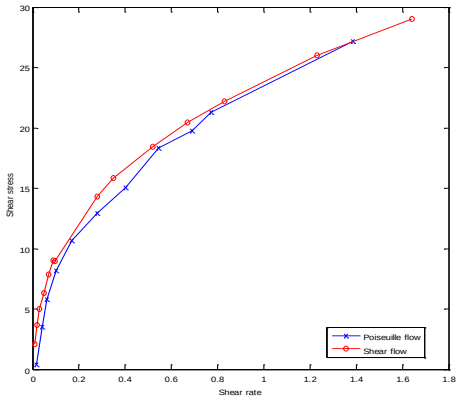

Figure 9: Shear stress versus shear rate calculated from shear flow (red$-o$) and Poiseuille flow (blue$-x$).

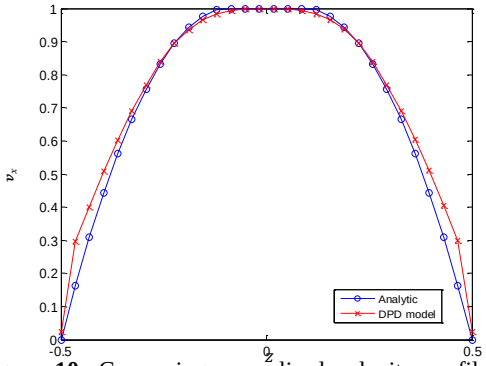

Figure 10: Comparing normalised velocity profile in a Poiseuille flow (red−x) with the analytical steady state solution for the Poiseuille flow of Bingham fluids (blue−o).

ACKNOWLEDGEMENT

We thank the National Research Foundation, Keppel Corporation and National University of Singapore for supporting this work done in the Keppel-NUS Corporate Laboratory. The conclusions put forward reflect the views of the authors alone, and not necessarily those of the institutions within the Corporate Laboratory.

REFERENCES

ARIENTI, M., PAN, W., LI, X., KARNIADAKIS, G., (2011), "Many-body dissipative particle dynamics simulation of liquid/vapor and liquid/solid interactions", *J. Chem. Phys.*, **134**(20), 204114.

BOEK, E. S., COVENEY ,P. V. , LEKKERKERKER, H. N. W. , VAN DER SCHOO, TP., (1997), "Simulating the rheology of dense colloidal suspensions using dissipative particle dynamics", *Phys. Rev. E*, **55**(3)**,** 3124-3133.

ESPAÑOL, P., REVENGA, M., (2003), "Smoothed dissipative particle dynamics", *Phys. Rev. E*, **67,** 026705.

FAN, X., PHAN-THIEN, N., CHEN, S., WU, X. NG, T.Y., (2006), "Simulating flow of DNA suspension using dissipative particle dynamics", *Phys Fluids*, **18**, 063102.

HOOGERBRUGGE, P.J., and KOELMAN, J.M.V.A., (1992), "Simulating microscopic hydrodynamic phenomena with dissipative particle dynamics", *Europhys. Lett*, **19**, 155.

IRVING, J. H., and J. G. KIRKWOOD, (1950), "The statistical mechanical theory of transport processes. IV. The equations of hydrodynamics," *J. Chem. Phys*. **18**, 817.

KOELMAN, J. M. V. A. AND HOOGERBRUGGE, P. J., (1993), "Dynamic Simulations of Hard-Sphere Suspensions under Steady Shear", *EPL (Europhys Letters)*, **21**(3), 363.

LI W., OUYANG J. and LIU Q., (2015), "An efficient DPD-based algorithm for simulating ferromagnetic colloidal suspensions", *ASME. J. Comput. Nonlinear Dynam*, **11**(2):024501-024501-6.

LIU, M., MEAKIN, P. and HUANG, H., (2006), "Dissipative particle dynamics with attractive and repulsive particle-particle Interactions", *Phys. Fluids*, 18, 017101.

LIU, M., MEAKIN, P. and HUANG, H. (2007), "Dissipative particle dynamics simulation of multiphase fluid flow in micro-channels and microchannel networks", *Phys. Fluids*, **19**, 033302.

MAI-DUY, N., PAN, D., PHAN-THIEN, N. and KHOO, B.C., (2013). "Dissipative particle dynamics modelling of low Reynolds number incompressible flows", *J. Rheology*, **57**, 585-604.

MAI-DUY, N., PHAN-THIEN, N. and KHOO, B.C., (2013), "A numerical study of strongly overdamped Dissipative Particle Dynamics (DPD) systems", *J. Comp. Physics*, **245**, 150–159.

MAI-DUY, N. , PHAN-THIEN, N. and KHOO, B.C., (2015), "Investigation of particles size effects in Dissipative Particle Dynamics (DPD) modelling of colloidal suspensions", *Comput. Phys. Commun.*, **189**, 37–46.

MARSH, C., (1998), "Theoretical aspects of dissipative particle dynamics", *PhD Thesis*, University of Oxford.

MOEENDARBARY, T. Y. NG and ZANGENEH, M. (2010), "Dissipative Particle Dynamics in soft matter and polymeric applications - a review", *Int. J. Appl. Mech.*, **2**(1), 161–190.

PAN, D., PHAN-THIEN, N. and KHOO, B.C., (2014), "Dissipative particle dynamics simulation of droplet suspension in shear flow at low Capillary number", *J. Non-Newton Fluid Mech.*, **212**, 63-72.

PAPANASTASIOU, T.C, (1987) "Flows of materials with yield, *J. Rheol*., 385-404.

PAN, W., B. CASWELL and G. E. KARNIADAKIS (2010), "Rheology, microstructure and migration in Brownian colloidal suspensions," *Langmuir*, 26, 133.

PHAN-THIEN, N., (2013), "Understanding Viscoelasticity - An Introduction to Rheology", Edition Number 2, *Springer-Verlag Berlin Heidelberg.*

PHAN-THIEN, N., MAI-DUY, N., and KHOO, B.C. (2014), "A Spring Model for Suspended Particles in Dissipative Particle Dynamics", *J. Rheology*, **58**(4), 839-867.

PIVKIN, I.V., CASWELL, B. and KARNIADAKIS, G. EM, (2011), "Dissipative Particle Dynamics", *Rev. Comp. Ch*., **27**, 85- 110.

SEVINK, G. J. A., and FRAAIJE, J. G. E. M., (2014), "Efficient solvent-free dissipative particle dynamics for lipid bilayers", *J. Soft Matter*, **10**(28), 5129-5146.

TRAN-DUC, T., PHAN-THIEN, N. and KHOO, B.C. (2013), "Rheology of Bubble Suspensions Using Dissipative Particle Dynamics. Part I. A Hard-Core DPD Particle Model for Gas Bubbles", *J. Rheology*, **57**(6), 1715-1737.

WARREN, P. B., (2003), "Vapor-liquid coexistence in many-body dissipative particle dynamics", *Phys. Rev. E*, **68**, 066702.

